

Article

Barium Hydroxide Nanoparticle–Phosphoric Acid System for Desalination and Consolidation of Tomb Murals

Yan Rong ^{1,*}, Jinglong Yang ², Siping Huang ¹ and Yuhu Li ³¹ College of History and Culture, Xianyang Normal University, Xianyang 712099, China² Xianyang Cultural Relics Protection Center, Xianyang 712099, China³ Engineering Research Center of Historical Cultural Heritage Conservation, Ministry of Education, School of Materials Science and Engineering, Shaanxi Normal University, Xi'an 710119, China

* Correspondence: rongyan@xync.edu.cn or allenry@126.com

Abstract: Tomb murals are an important component of cultural heritage, but the extant majority of burial murals are severely damaged. There are various causes behind the deterioration of tomb murals, among which the detrimental effects of sodium sulfate on murals are some of the most difficult to treat. In the past decades, the application of alkaline earth metal hydroxides (such as Ba(OH)₂, Ca(OH)₂, and Ma(OH)₂) for the conservation and consolidation of murals has become more common. However, there are some problems, such as large particles, poor permeability, and potential for surface whitening. In response to this issue, we investigated a facile method for the synthesis of nano barium hydroxide (N-Ba(OH)₂), from which we developed a barium hydroxide nanoparticle–phosphoric acid (N-Ba(OH)₂/H₃PO₄) multisite in situ consolidation system. The results show that N-Ba(OH)₂/H₃PO₄ consolidation material has good permeability and mechanical properties compared with commercial Ba(OH)₂ and other common consolidation materials. This material performs very well in both salt resistance and desalination tests, the color difference change is minimal, and the technique is suitable for the practical manipulation of outdoor artifact conservation work. Recently, it has even been used in the desalination and consolidation of tomb murals in Jiangxi, China, the results of which opened a new way of thinking about the long-term conservation of tomb murals.

Keywords: cultural heritage; sodium sulfate; hydroxide nanoparticles–phosphoric acid; consolidation; tomb murals



Citation: Rong, Y.; Yang, J.; Huang, S.; Li, Y. Barium Hydroxide Nanoparticle–Phosphoric Acid System for Desalination and Consolidation of Tomb Murals. *Crystals* **2022**, *12*, 1171. <https://doi.org/10.3390/cryst12081171>

Academic Editor: Claudia Scatigno

Received: 7 August 2022

Accepted: 18 August 2022

Published: 20 August 2022

Publisher's Note: MDPI stays neutral with regard to jurisdictional claims in published maps and institutional affiliations.



Copyright: © 2022 by the authors. Licensee MDPI, Basel, Switzerland. This article is an open access article distributed under the terms and conditions of the Creative Commons Attribution (CC BY) license (<https://creativecommons.org/licenses/by/4.0/>).

1. Introduction

Tomb murals are an important branch of mural cultural heritage. Ancient tomb murals in China are mainly composed of a support, mortar layer, lime layer, and pigment layer (Figure 1). The support is generally a brick structure, while the mortar layer [1] is typically composed of soil and wheat straw, which may contain a small amount of sand. The lime layer is primarily composed of calcium carbonate, a product created as a result of the reaction of lime (calcium hydroxide) upon exposure to carbon dioxide in the air. The outermost pigment layer is painted on the surface of the lime layer by mixing animal adhesive [2,3] and mineral pigment [4,5]. After tomb murals are excavated, they are affected by environmental temperature and humidity, soil water content, soluble salt distribution, and other factors, especially harm caused by sulfate [6]. Due to the capillary effect of water evaporation, a large amount of sulfate solution is brought to the surface of the pigment layer. With the change in environment, sulfate repeatedly dissolves and crystallizes in this process, and the volume continuously expands and shrinks. Finally, the murals will appear powdery [7]. If a mural in these conditions is not conserved in time, it will eventually lose its original artistic, historical, and scientific value.

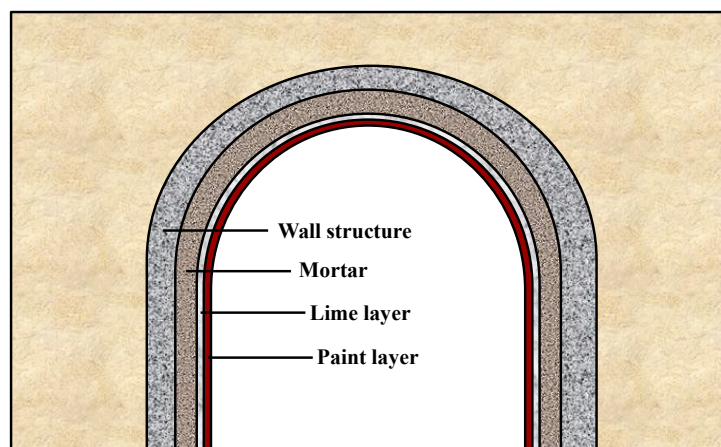


Figure 1. Structure diagram of tomb mural.

At present, many inorganic as well as organic materials are used in the conservation of murals. In the 20th century, organic materials were most widely used because of their excellent adhesion and low cost [8,9]. For example, Paraloid B72 [10,11] and Paimal AC33 [12] polymers were introduced and widely used in the conservation practices of cultural heritage in the 1970s. However, after decades of extensive use, these materials have shown their limitations and defects. One issue is that organic materials are inconsistent with the porous structure of the pigment layer, resulting in changes in air permeability and water permeability from the original structure [13,14]. In addition, changes in organic materials over time cause the synthetic resin to become crosslinked, broken, and discolored, thus ultimately losing its original adhesiveness [15,16]. Therefore, these products not only lose their function as consolidation materials, but their very presence on the surface of the murals has also often become the root cause of their deterioration. Inorganic materials can solve these problems, and traditional lime water treatment methods are usually more physically and chemically compatible with murals. However, due to their large particle size, low solubility in water, poor permeability, minimal contact area with air, and low utilization rate, it is easy for lime particles to accumulate on the surface of murals and form white areas [17,18].

In light of these problems, this paper studies a desalination and consolidation method using an N-Ba(OH)₂/H₃PO₄ system for tomb murals in sulfate-rich environments (Figure 2a). This method is currently used to protect tomb murals in Jiangxi, China (Figure 2b). First, when phosphoric acid is added, all of the divalent and above divalent soluble metal salt ions in the mural are transformed into insoluble precipitates. This means that the divalent and above metal cations in the mural form phosphate precipitates, which are attached to the microporous structure of the mural. This precipitation layer plays a role in desalination and consolidation while also enhancing the pigment's stability. Theoretically, the following reactions may occur:



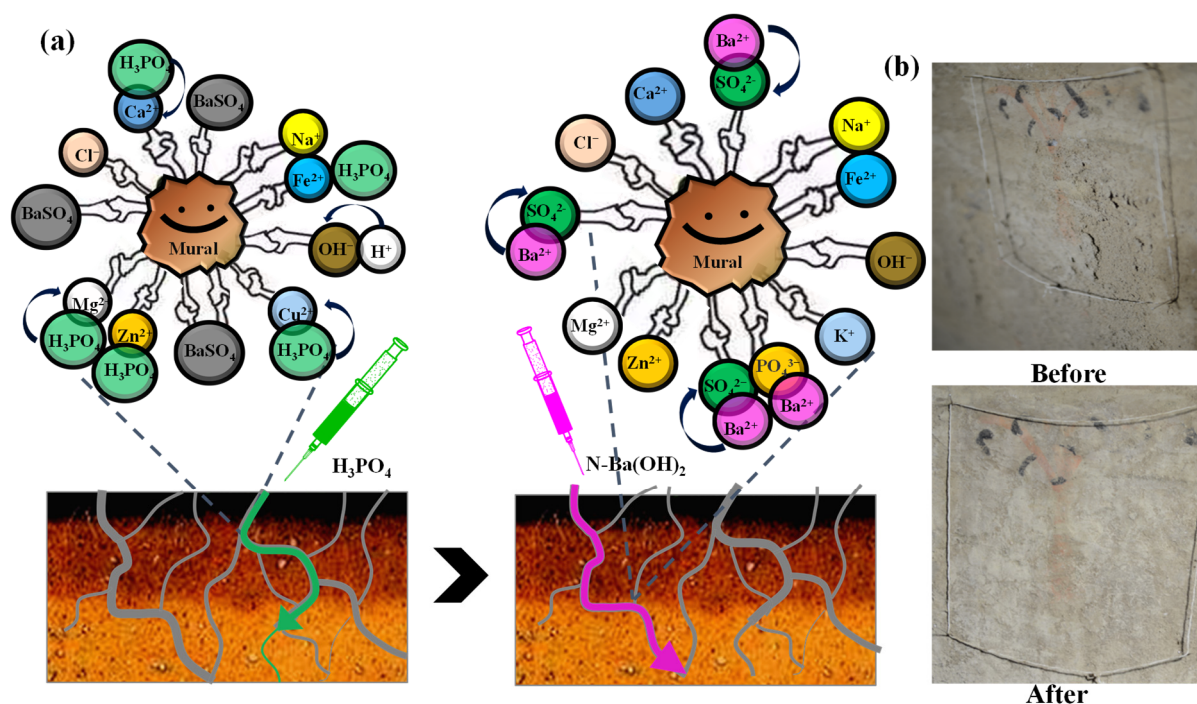
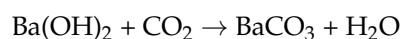
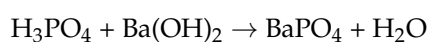


Figure 2. (a) Reaction mechanism of desalination and consolidation of tomb murals. (b) Application to tomb murals in Jiangxi, China.

In the second step, a solution of barium hydroxide nanoparticles is added to the mural [19]. The solution can be added in excess to ensure a complete reaction. All sulfate ions in the soluble salt are transformed into barium sulfate precipitate to fully mineralize it. The excess phosphoric acid from the first step reacts to produce barium phosphate precipitate, and finally, excess barium hydroxide nanoparticles react with carbon dioxide in the air to produce barium carbonate precipitate.



After the above comprehensive reaction, all divalent and above metal ions and sulfate ions in the mural are transformed into insoluble sulfate and phosphate precipitates, which can desalinate and consolidate the microporous structure attached to the mural. The innovation of this paper has two aspects:

- At present, most of the existing methods for synthesizing barium hydroxide nanoparticles need to be completed in a laboratory. However, the barium hydroxide nanoparticles described in this paper can be directly synthesized in the field, which is convenient for field construction.
- In the proposed method, a weak acid is first used to remove the divalent metal ions in murals, eliminating the means by which it produces soluble salts, and then barium hydroxide nanoparticles are used to convert sulfate and carbonate into mineral precipitate. The excess barium hydroxide can also be converted into barium carbonate precipitate.

2. Materials and Methods

2.1. Materials

Phosphoric acid, ammonium hydroxide aqueous solution, barium chloride, barium hydroxide, ethanol, and methanol were purchased from Sinopharm Chemical Reagent

Co., Ltd. (Shanghai, China). The pigments (ultramarine, cinnabar, and malachite) were purchased from Beijing Tianya Pigment Co., Ltd (Beijing, China).

2.2. Preparation of the Materials

We summarized the full names and abbreviations of the materials in this paper (Table 1).

Table 1. Full names and abbreviations of the materials.

Full Name	Abbreviation
Barium hydroxide nanoparticles	N-Ba(OH) ₂
Commercial barium hydroxide	M-Ba(OH) ₂
Barium hydroxide nanoparticles–phosphoric acid system (N-Ba(OH) ₂ /H ₃ PO ₄)	PB
70/30% mixture of poly (ethyl methacrylate-methacrylate)	B72

2.2.1. PB

A total of 2 mL of phosphoric acid was placed in 1000 mL of ethanol and then stirred until completely dissolved to form a colorless transparent solution; this was recorded as material P. Then, 24 g of barium chloride and 16 mL of ammonium hydroxide were added to 1000 mL of methanol and stirred at room temperature to prepare barium hydroxide nanoparticles; this was recorded as material B. Each time the simulated sample was consolidated, 5 ml of material P was removed with a needle tube for reinforcement treatment. After natural drying, 10 mL of material B was removed with a needle tube for reinforcement treatment. This kind of consolidation material was recorded as PB.

2.2.2. Commercial Barium Hydroxide

Barium hydroxide is easily soluble in methanol at high temperatures. Thus, in the next step, 15 g of barium hydroxide was placed into a 1000 mL three-port flask, and 500 mL of methanol was added. The solution was refluxed and dissolved for 4 h under the condition that the oil bath temperature was maintained at 75 °C. After cooling the temperature, barium hydroxide was diluted according to a volume ratio of 1:2 to form a stable solution, which was sealed to avoid contact with air. The resulting material was recorded as M-Ba(OH)₂.

2.2.3. B72

B72 powder was dissolved in acetone and prepared in a solution with a B72 content of 5%. This was recorded as B72.

2.2.4. Simulated samples

The preparation of simulated mural samples (Figure 3) was carried out as follows:

Step 1: The selected wheat straw was mixed with 80 mesh of selected soil samples and added to distilled water.

Step 2: The sample block was collected and cut into a 5 cm × 5 cm × 5 cm black brick. It was then soaked in a culture dish containing distilled water.

Step 3: The wheat straw was mixed with mud and coated on the bricks (about 1 cm thick).

Step 4: Next, 100 g of calcium hydroxide was dissolved in 50 mL of distilled water, and the prepared lime water was applied to the surface of the simulated mural sample.

Step 5: Finally, 3% gelatin and mineral pigments were applied to the surface of the simulated sample; the simulated mural sample was complete after drying.

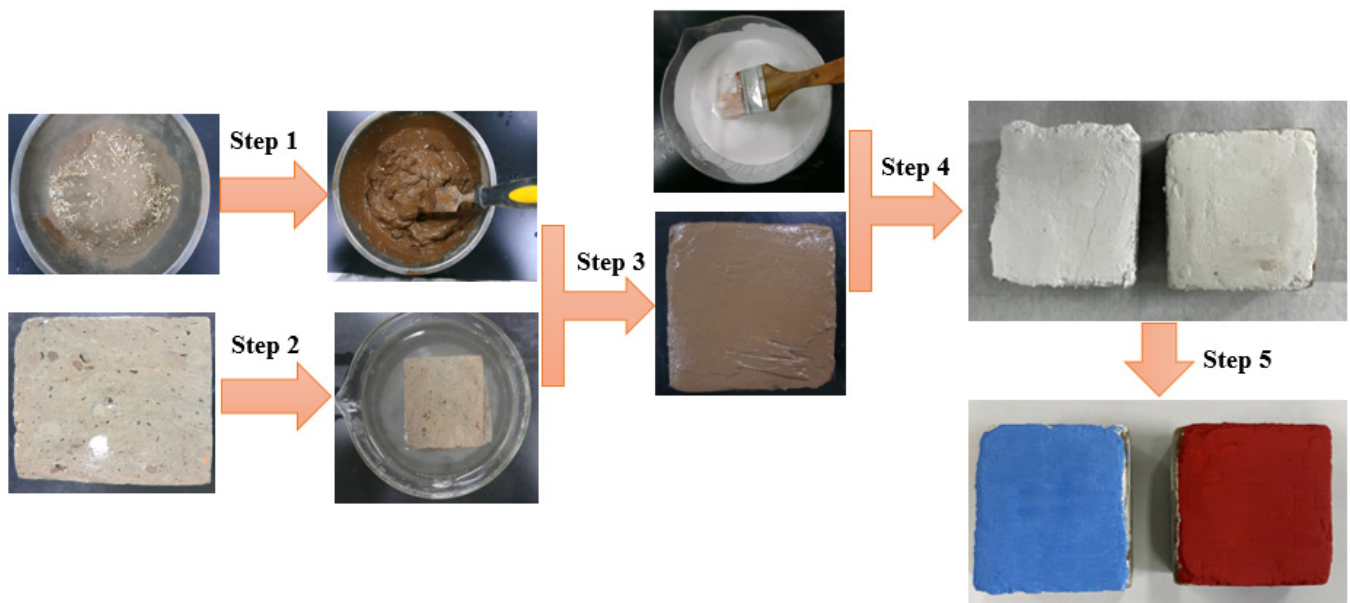


Figure 3. Production process of simulated mural sample block.

2.3. Test Methods

2.3.1. Physical Test

The structure and morphology of the sample were physically characterized by X-ray diffraction (XRD, D/max-Rc, Rigaku, Tokyo, Japan) and transmission electron microscopy (TEM, FEI, Tecnai G2 F20, Portland, OR, USA).

2.3.2. Penetration Depth Test

Two green bricks were consolidated with PB and M-Ba(OH)₂ materials by the drip infiltration method and cut along the drip infiltration direction. Samples were taken at 0, 1, 2, 3, 4, and 5 cm away from the surface of the profile. The content of barium was measured by an Inductively Coupled Plasma Emission Spectrometer (ICP, LEEMAN LABS INC., Hudson, NH, USA), model pridigy7, wavelength range 165 nm–1100 nm, resolution 0.007 nm, and detection limit 5–100 ppb) to explore the penetration depth of consolidation materials.

2.3.3. Color Difference Test [20,21]

During our study, the CIE ΔL , Δa , and Δb color coordinate system was used. The simulated samples were treated with three kinds of reinforcement materials. The color change was characterized according to the change in brightness ΔL , the red–green difference Δa , the yellow–blue difference Δb , and the calculation of the color difference ΔE before and after the reinforcement of the simulated samples. The following formula was used to calculate the difference in color values:

$$\Delta E = \sqrt{(\Delta L)^2 + (\Delta a)^2 + (\Delta b)^2}$$

2.3.4. Compressive Strength Test

The simulated samples were placed on a QT-1136PC universal material testing machine (Guangdong Gaotai Co., Ltd., China). The maximum breaking force of the simulated samples was determined through the program setting's constant moving load method, and the compressive strength of the simulated samples treated and untreated with three

different kinds of consolidation materials was calculated. The formula for calculating compressive strength is as follows:

$$P = 10^{-2}F/S$$

where P is the compressive strength (MPa), F is the total yield stress (N), and S is the simulated sample area (cm^2).

2.3.5. Scotch Tape Test (STT) [22]

This is a research method used to characterize the consolidation efficiency by simulating the surface loss mass change (STT) of the mural samples. Transparent tape was cut into a square with the same size as the simulated sample block ($5 \text{ cm} \times 5 \text{ cm}$) and attached to the surface of the simulated sample block. Then, the transparent tape was torn off with tweezers at a constant speed. The same method was repeated 3 times for each sample to find the average value. The mass loss rate was calculated using the following formula:

$$\text{Weight loss} = \frac{m_2 - m_1}{a^2}$$

where m_1 and m_2 represent the weight of the square tape and the weight of the square tape after it has been removed from the painting surface, respectively, and a is the length and width of the scotch tape.

2.3.6. Salt Resistance and Desalination Test

Salt Resistance Test [20]

Soluble salt/pigment/consolidation system (the soluble salt itself exists in the sample): ultramarine, cinnabar, and malachite pigments were mixed with 5% soluble salt (Na_2SO_4) and gelatin solution and brushed onto the prepared lime layer. Finally, the consolidation materials were dropped onto samples, which were placed at room temperature for 24 h. All the samples were put into a freeze–thaw circulation box with a temperature set to $-40 \text{ }^\circ\text{C}$ – $40 \text{ }^\circ\text{C}$ and humidity set to 50%. The samples were left in the circulation box for 60 days, conducting an STT test every 15 days.

Desalination Property Test

Firstly, the original salt in the black bricks was removed. The specific operations are as follows: four samples of black bricks with the same material were taken and put into a beaker containing deionized water; the beaker was placed in an ultrasonic cleaner, and the removal of soluble salt in the black bricks was monitored by testing the conductivity of the aqueous solution in the beaker. After constantly changing the deionized water in the beaker, when the conductivity value tended to be stable, it was considered that the salt removal of the black bricks was completed. After desalting, the black bricks were dried at room temperature.

Secondly, 5% sodium sulfate solution was prepared. The permeable stone was placed in a Petri dish containing 10 mL of sodium sulfate solution, and the demineralized black brick was placed on the permeable stone. Through the capillary action of the permeable stone, the salt solution was transferred to the black brick and then left to stand for 30 min before drying. This process was used to simulate the water and salt migration in murals (Figure 4).

PB was added dropwise to the black brick sample containing sodium sulfate, and three reference samples (M-Ba(OH)_2 , B72, and untreated) were prepared by the same method and left to stand at room temperature for 72 h. The ion concentrations of Ca^{2+} , Mg^{2+} , Na^+ , SO_4^{2-} , NO_3^- , and Cl^- in the four samples were tested by ion chromatography. Specifically, the four black bricks were cut from the middle, and the powder samples were scraped from 0, 2, and 4 cm away from the surface. All powder samples were dried at $105 \text{ }^\circ\text{C}$ and ground with a mortar, and 0.1 g of each sample was weighed and dissolved in 10 mL of ultra-pure

water (resistivity 18.2 M Ω /cm). The beaker was subjected to ultrasound for 30 min. Then, the solution was poured into a 25 mL centrifuge tube, centrifuged at a speed of 8000 r/min for 10 min, and then passed through a 45 μ m filter head for machine testing. With the ion chromatograph (Diane, Sunnyvale, CA, USA, model ICS-90/1000), the anion and cation concentrations in the solution were tested to reflect the desalination performance of the reinforcement material.

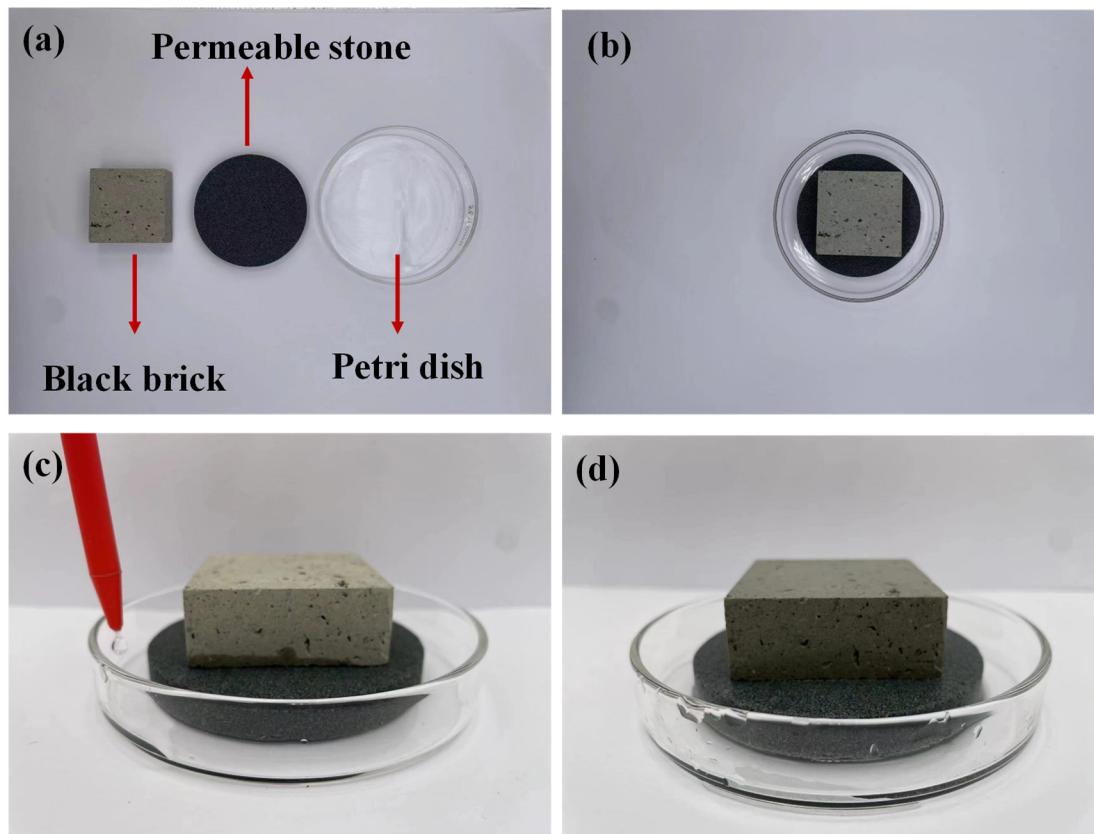


Figure 4. (a) Black bricks, permeable stones, and Petri dishes. (b) The permeable stone was placed in the Petri dish, and the black brick was placed on the pervious stone. (c) Ten milliliters of 5% sodium sulfate solution was dropped into the Petri dish. (d) After standing for 30 min, water and salt were transported to the brick by capillary action of the permeable stone.

3. Results

3.1. Penetration Depth of $N\text{-Ba(OH)}_2$ and $M\text{-Ba(OH)}_2$

Previous studies have shown that the growth morphology of inorganic nanomaterials can be adjusted by controlling the electrolytic dissociation rate. Specifically, a weak electrolyte with a relatively low ionization constant as a reactant is more likely to lead to one-dimensional product growth, which is conducive to the control of the product's particle size [23]. In this experiment, we selected barium hydroxide produced by the reaction of ammonium hydroxide aqueous solution with barium chloride as a reactant. After preparation, a TEM comparison showed that the particle size of $N\text{-Ba(OH)}_2$ was only about 8 nm and the size distribution was uniform (Figure 5a), while $M\text{-Ba(OH)}_2$ had micron-sized bulk (Figure 5b). The decrease in particle size greatly improved the solubility, permeability, and usability of barium hydroxide. Compared with $M\text{-Ba(OH)}_2$, $N\text{-Ba(OH)}_2$ greatly reduced the change of color difference and provided better reinforcement.

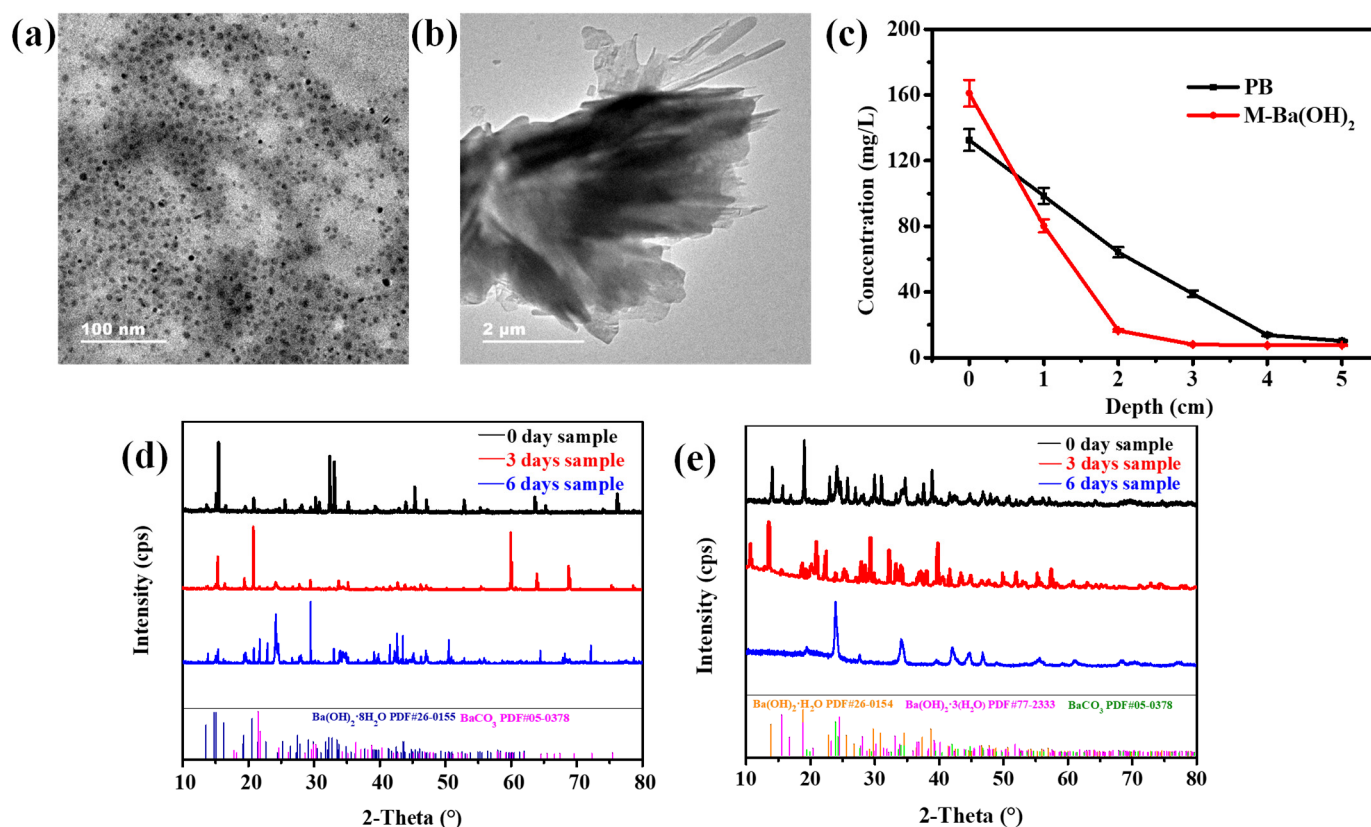


Figure 5. (a) TEM of N-Ba(OH)₂ nanoparticles; (b) TEM of M-Ba(OH)₂ particles; (c) penetration depth of barium ions after the black brick sample was left standing for 2 h; (d) XRD of M-Ba(OH)₂ at 0, 3, and 6 days; and (e) XRD of N-Ba(OH)₂ at 0, 3, and 6 days.

In order to further explore the influence of barium hydroxide's particle size on penetration, the penetration depths of N-Ba(OH)₂ and M-Ba(OH)₂ when applied for reinforcement were characterized using the ICP detection method (Figure 5c). At 0 cm from the surface, the barium ion content of the sample treated with M-Ba(OH)₂ was 161 mg/L, while the barium ion content of the sample treated with N-Ba(OH)₂ was 132.5 mg/L. The prevalence of M-Ba(OH)₂ on the surface was due to its large particles and poor permeability. In the 2 cm–5 cm range, the barium ion concentration of the sample treated with M-Ba(OH)₂ decreased rapidly, while the barium ion concentration at 3–5 cm was below 10 mg/L. The barium ion concentration of the sample treated with N-Ba(OH)₂ decreased gradually with the increase in depth. The barium ion concentration at 5 cm remained at 10.2 mg/L, indicating that M-Ba(OH)₂ can only penetrate to about 2 cm during reinforcement, while the penetration of N-Ba(OH)₂ can reach about 5 cm. This has positive significance for the long-term preservation of murals. If the reinforcement material is enriched on the surface of the mural and does not have good permeability, it can easily cause flaking on the mural's surface. This is because the surface strength is greater than that of the interior, which remains powdered. This situation can eventually lead to secondary damage to the mural.

Finally, we characterized the carbonization time of the two barium hydroxide particles by XRD (Figure 5d,e). After N-Ba(OH)₂ and M-Ba(OH)₂ were dispersed in methanol, they were deposited on drop-loaded glass slides and then carbonized in a wet chamber with a relative humidity of 23 ± 2 °C and $50 \pm 5\%$. Every three days, XRD was measured for these materials. For the N-Ba(OH)₂ materials, two crystalline barium hydroxide nanoparticles (Ba(OH)₂·H₂O and Ba(OH)₂·3H₂O) were synthesized. When left for 3 days, the peak of barium hydroxide became weak, and the peak of barium carbonate gradually appeared, indicating that part of barium hydroxide had been transformed into barium carbonate. After being left for 6 days, all of the peaks of barium hydroxide had disappeared and

transformed into barium carbonate. For M-Ba(OH)₂ material, there was no peak of barium carbonate in 0–3 days, only the peak of Ba(OH)₂·8H₂O. After 6 days, the peak of barium carbonate slowly appeared. In conclusion, compared with M-Ba(OH)₂, N-Ba(OH)₂ material has a shorter carbonization time and a better penetration effect.

3.2. Mechanical Property Test

Improving the strength of murals is the primary problem that is solved by reinforcement materials. To test the strength, we used a universal material testing machine to compare the compressive strength of the simulated sample at 7 and 28 days after treatment with three kinds of consolidation materials (Figure 6a). The compressive strength of the untreated sample was 2.34 MPa. The compressive strength of the three reinforcement materials increased compared with the untreated sample. The compressive strengths of M-Ba(OH)₂ and PB were higher than that of B72. At 7 days, the compressive strengths of M-Ba(OH)₂ and PB remained basically the same, but after 28 days, the compressive strength of PB increased to 5.13 MPa, an increase of about 34% when compared with M-Ba(OH)₂. We also conducted the transparent tape test “STT” (Figure 6b) to evaluate the bonding strength between pigment particles and consolidation materials. The results show that for untreated samples, the mass loss was 2.23 mg/cm². The mass losses of the samples treated with PB, M-Ba(OH)₂, and B72 reinforcement were 1.21 mg/cm², 1.95 mg/cm², and 0.81 mg/cm², respectively. The mass lost from the sample treated with PB was about 37% less than that of the M-Ba(OH)₂ sample, which further proves that PB has the ability to enhance the bonding strength of murals.

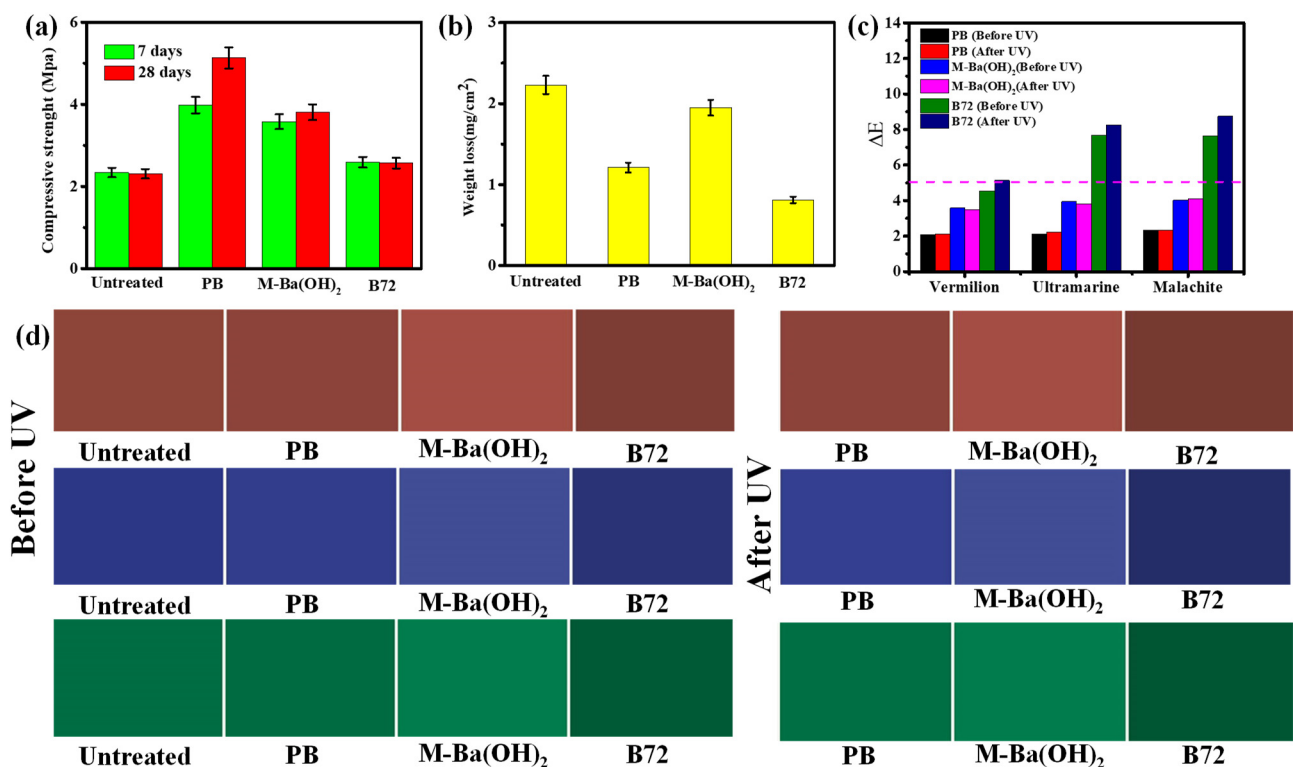


Figure 6. (a) Compressive strength test of simulated samples treated with PB, M-Ba(OH)₂, and B72 at 7 and 28 days; (b) the weight loss of simulated samples treated with PB, M-Ba(OH)₂, and B72 after curing in STT; (c) CIELAB ΔE changes in ultramarine, cinnabar, and malachite pigments treated with PB, M-Ba(OH)₂, and B72 before and after UV aging; and (d) color change pictures of simulated samples treated with PB, M-Ba(OH)₂, and B72 before and after UV aging.

While B72 did not perform as well as M-Ba(OH)₂ and PB during the compressive strength test, it performed quite well in the STT test, resulting in a loss of only 0.81 mg/cm².

This is because B72 is only able to consolidate the surface but cannot create overall consolidation. A side view of the sample shows that B72's penetration was poor, and only the surface pigment layer was consolidated. The compressive strength values of PB and M-Ba(OH)₂ were both higher than those of B72 and the untreated samples. However, the compressive strength of PB continued to increase after 7 days, while the basic protection provided by M-Ba(OH)₂ remained unchanged. This is because the barium hydroxide nanoparticles were small, so the penetration of the simulated sample was deep, and the carbonation rate increased. In addition, the PB material was added with phosphoric acid, which caused some divalent cations to precipitate in the microporous structure of the simulated sample. As a result, the overall compressive strength increased.

3.3. Color Difference Performance

The color difference directly affects whether the surface of the mural's pigment layer protected by consolidation material can maintain its original appearance, making it an important criterion for the application of consolidation and conservation materials. In this study, a color difference standard of ΔE equal to 5 was selected as the critical value of an acceptable color difference change [24]. The test data (Figure 6c) compare the color difference changes in ultramarine, cinnabar, and malachite in the simulated samples treated with different consolidation materials. The ultramarine and simulated malachite samples treated with B72 exceeded the critical value of 5, but compared to the untreated samples, ΔL decreased significantly, and the color became dark (Figure 6d). The three pigments treated with M-Ba(OH)₂ increased in ΔL and brightened in color compared with the untreated sample (Figure 5d). This is because the M-Ba(OH)₂ particles were large and could not effectively penetrate, resulting in their accumulation and whitening on the surface. The treatment that resulted in the least change in color was PB: the changes were found to be 2.07, 2.11, and 2.32 (cinnabar, ultramarine, and malachite, respectively). Then, the color difference changes in the materials under the action of ultraviolet light were explored. The samples treated with three materials were placed under a 254 MM UV lamp. The ultraviolet wavelength of the ultraviolet aging test chamber was 313 nm, and the intensity was 0.8 W/m². After aging for 7 days, the color difference was evaluated. The test results show (Figure 6d,e) that the color of B72 continued to darken under UV aging. The Δe values of cinnabar, lapis lazuli, and malachite green pigments were 5.13, 8.25, and 8.74, respectively. PB and M-Ba(OH)₂ were hardly affected by UV aging, and the color difference ΔE was basically the same as that at the beginning, indicating that the organic materials were greatly affected by UV, while inorganic materials were relatively stable and less affected by UV.

3.4. Salt Resistance and Desalination Tests

We studied the soluble salt/pigment/consolidation system of each of the simulated samples (Figure 7a). After applying 5% soluble salt sodium sulfate to the untreated sample and subjecting it to 30 days of freeze–thaw cycles, there was a large area of flaking, which became loose and shapeless after 60 days. The simulated sample treated with B72 began to lose mass after 30 days, and the simulated samples appeared powdery after 60 days. The weight loss of the simulated samples after PB treatment was 4.59 mg/cm² at 45 days, more than two times less than that after M-Ba(OH)₂ treatment. At 60 days, the weight loss of PB was only 5.13 mg/cm², about thirteen times less than that of B72 and about four times less than that of M-Ba(OH)₂. This shows that PB treatment has good salt resistance. Due to the large particles and poor permeability of M-Ba(OH)₂, divalent cations were repeatedly combined with the remaining sulfate to form sulfate and destroy the pore structure. At 45 days, the pigment of the simulated samples treated with M-Ba(OH)₂ gradually began to fall off. B72 lost 1.95 mg/cm² in weight at 15 days due to its good consolidation efficiency, but the weight loss began to increase exponentially at 30 days due to its lack of salt resistance.

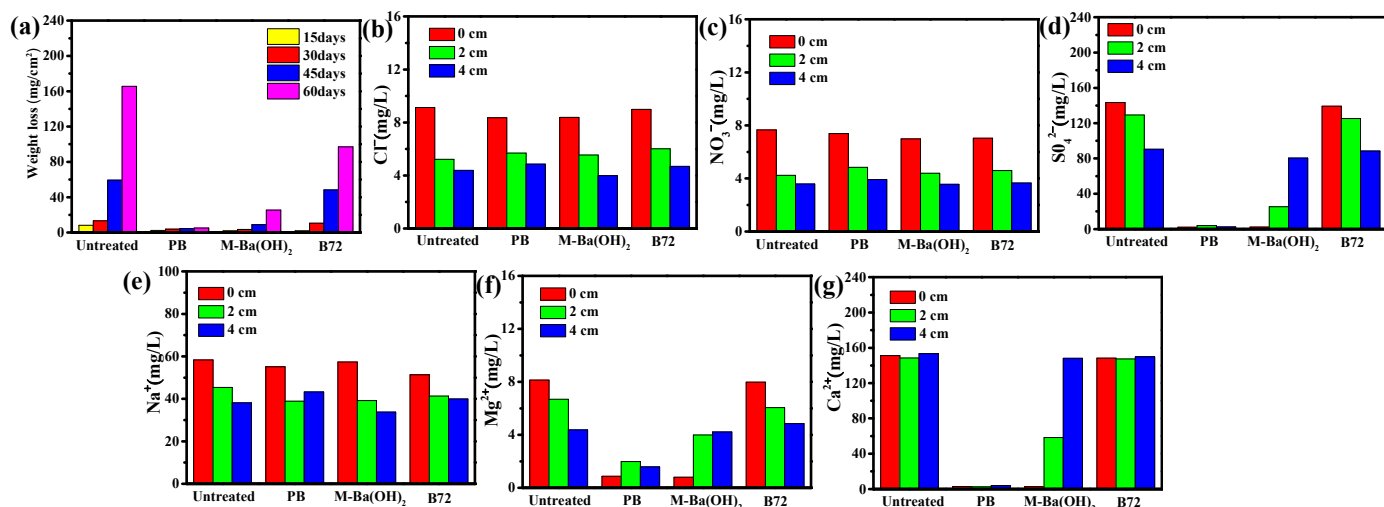


Figure 7. (a) Weight loss of simulated samples of soluble salt/pigment/consolidation system after PB, M-Ba(OH)₂, and B72 treatment. The concentrations of (b) chloride ions, (c) nitrate ions, (d) sulfate ions, (e) sodium ions, (f) magnesium ions, and (g) calcium ions in the simulated samples after PB, M-Ba(OH)₂, and B72 treatment.

According to the desalination performance test results (Figure 7b–g), the chloride ions, nitrate ions, and sodium ions at 0–4 cm were mostly unaffected by treatment when compared with the untreated samples. The sulfate ion concentrations on the surface of PB and M-Ba(OH)₂ were 2.1834 mg/L and 2.2481 mg/L, respectively, which are significantly reduced compared with the untreated samples, indicating that there is indeed a desalination effect. At 2 cm and 4 cm, the sulfate ion concentrations in the PB-treated sample were 3.9218 mg/L and 2.3641 mg/L, and the sulfate ion concentrations in M-Ba(OH)₂ were 25.2813 mg/L and 80.3952 mg/L, indicating that the sulfate ions in the simulated sample still existed below the surface due to the insufficient penetration depth of M-Ba(OH)₂. These results show that the treatment only creates surface consolidation, which is consistent with the salt tolerance test results. Meanwhile, compared with M-Ba(OH)₂ and untreated samples, the sulfate concentration in the PB-treated samples decreased significantly. At the same time, the contents of cationic calcium and magnesium ions also decreased due to the addition of phosphoric acid, which limited the reformation of divalent salts. B72 had basically no desalination performance, and the simulated sample still contained a large amount of sodium sulfate. Therefore, the weight loss after 15 days of the salt tolerance test was basically the same as that of the untreated sample.

4. Conclusions

In conclusion, our research demonstrates a simple and economical method for the consolidation of murals containing sodium sulfate. The divalent metal ions in murals are removed by phosphoric acid, and the means of generating soluble salts are eliminated. Then, barium hydroxide nanoparticles are used to convert sulfate and carbonate into mineral precipitate. Finally, the excess barium hydroxide nanoparticles can also be converted into barium carbonate precipitate, which plays a role in desalination and consolidation. According to the performance comparison experiment with M-Ba(OH)₂ and B72 materials, the PB material has good mechanical properties, desalination effect, and small color difference change. Its excellent performance is mainly due to the small barium hydroxide nanoparticles, deep penetration, and high carbonation rate. In addition, the barium hydroxide nanoparticles described in this paper can be directly synthesized outdoors, which is convenient for the conservation of outdoor murals. Its application in a mural protection field experiment in Jiangxi, China, had a significant effect, which provides a new idea for the conservation of murals containing sulfate.

Author Contributions: Conceptualization, Y.R. and Y.L.; methodology, J.Y.; investigation, S.H.; resources, Y.L.; data curation, Y.R.; writing—original draft preparation, Y.R. All authors have read and agreed to the published version of the manuscript.

Funding: This research was sponsored by the Shaanxi Social Science Foundation Project (2021G008); Key projects of Shaanxi Provincial Department of Education (17JZ080); Key cultivation and scientific research projects of Xianyang Normal University (XSYK21035); and “Blue talents” project of Xianyang Normal University (XSYQL201903) and supported by “Academic Leader” of Xianyang Normal University (XSYXSDT202114).

Institutional Review Board Statement: Not applicable.

Informed Consent Statement: Not applicable.

Data Availability Statement: All data included in this study are available upon request by contact with the corresponding author. Correspondence: rongyan@xync.edu.cn or allenry@126.com.

Acknowledgments: The authors thank Yu-Hu Li of Shaanxi Normal University for providing a small-scale application pilot for tomb murals and Jing-Long Yang for setting up the framework of the entire project. The authors are grateful for the funding support.

Conflicts of Interest: The authors declare no conflict of interest.

References

1. Hu, K.; Bai, C.; Ma, L.; Ke, B.; Liu, D.; Fan, B. A study on the painting techniques and materials of the murals in the five northern provinces' assembly hall, Ziyang, China. *Herit. Sci.* **2013**, *1*, 18. [[CrossRef](#)]
2. Song, Y.; Gao, F.; Nevin, A.; Guo, J.; Zhou, X.; Wei, S.; Li, Q. A technical study of the materials and manufacturing process used in the gallery wall paintings from the jokhang temple, tibet. *Herit. Sci.* **2018**, *6*, 18. [[CrossRef](#)]
3. Zhang, Y.; Wang, J.; Liu, H. Integrated Analysis of Pigments on Murals and Sculptures in Mogao Grottoes. *Anal. Lett.* **2015**, *48*, 2400–2413. [[CrossRef](#)]
4. Li, Z.; Wang, L.; Ma, Q.; Mei, J. A scientific study of the pigments in the wall paintings at jokhang monastery in lhasa, Tibet, China. *Herit. Sci.* **2014**, *2*, 21. [[CrossRef](#)]
5. Li, J.; Wan, X.; Bu, Y.; Li, C.; Liang, J.; Liu, Q. In situ identification of pigment composition and particle size on wall paintings using visible spectroscopy as a noninvasive measurement method. *Appl. Spectrosc.* **2016**, *70*, 1900–1909. [[CrossRef](#)]
6. Li, F.; Wang, X.; Guo, Q.; Zhang, B.; Pei, Q.; Yang, S. Moisture adsorption mechanism of earthen plaster containing soluble salts in the mogao grottoes of China. *Stud. Conserv.* **2018**, *64*, 159–173. [[CrossRef](#)]
7. Jia, Q.; Chen, W.; Tong, Y.; Guo, Q. Experimental study on capillary migration of water and salt in wall painting plaster: A case study at mogao grottoes, China. *Int. J. Arch. Herit.* **2022**, *16*, 705–716. [[CrossRef](#)]
8. Unoki, M.; Kimura, I.; Yamauchi, M. Solvent-soluble fluoropolymers for coatings—Chemical structure and weatherability. *Surf. Coatings Int. Part B Coat. Trans.* **2002**, *85*, 209–213. [[CrossRef](#)]
9. Artesani, A.; Di Turo, F.; Zucchelli, M.; Traviglia, A. Recent advances in protective coatings for cultural heritage—An overview. *Coatings* **2020**, *10*, 217. [[CrossRef](#)]
10. Fu, P.; Teri, G.; Chao, X.; LI, J.; Li, Y.; Yang, H. Modified Graphene-FEVE Composite Coatings: Application in the Repair of Ancient Architectural Color Paintings. *Coatings* **2020**, *10*, 1162. [[CrossRef](#)]
11. Murray, A. Materials for conservation: Organic consolidants, adhesives and coatings. *Stud. Conserv.* **2013**, *58*, 58–59. [[CrossRef](#)]
12. Zhang, Y.; Li, X.; Zhu, J.; Wang, S.; Wei, B. Hybrids of cnts and acrylic emulsion for the consolidation of wall paintings. *Prog. Org. Coat.* **2018**, *124*, 185–192. [[CrossRef](#)]
13. Chelazzi, D.; Dei, L. Physicochemical characterization of acrylic polymeric resins coating porous materials of artistic interest. *Prog. Org. Coat.* **2004**, *49*, 282–289.
14. Giorgi, R.; Baglioni, M.; Berti, D.; Baglioni, P. New methodologies for the conservation of cultural heritage: Micellar solutions, microemulsions, and hydroxide nanoparticles. *Acc. Chem. Res.* **2010**, *43*, 695. [[CrossRef](#)]
15. Lazzari, M.; Chiantore, O. Thermal-ageing of paraloid acrylic protective polymers. *Polymer* **2000**, *41*, 6447–6455. [[CrossRef](#)]
16. Baglioni, M.; Rengstl, D.; Berti, D.; Bonini, M.; Giorgi, R.; Baglioni, P. Removal of acrylic coatings from works of art by means of nanofluids: Understanding the mechanism at the nanoscale. *Nanoscale* **2010**, *2*, 1723–1732. [[CrossRef](#)]
17. Giorgi, R.; Ambrosi, M.; Toccafondi, N.; Baglioni, P. Nanoparticles for cultural heritage conservation: Calcium and barium hydroxide nanoparticles for wall painting consolidation. *Chem. Eur. J.* **2010**, *16*, 9374–9382. [[CrossRef](#)]
18. Chelazzi, D.; Poggi, G.; Jaidar, Y.; Toccafondi, N.; Giorgi, R.; Baglioni, P. Hydroxide nanoparticles for cultural heritage: Consolidation and protection of wall paintings and carbonate materials. *J. Colloid. Interf. Sci.* **2013**, *392*, 42–49. [[CrossRef](#)]
19. Kroftová, K.; Škoda, D.; Kuřitka, I.; Kubát, J. Technology of preparation of barium and magnesium hydroxide nanodispersion and possibilities of their use in monument care. *Acta Polytech. CTU Proc.* **2019**, *21*, 21–23. [[CrossRef](#)]

20. Bourguignon, E.; Tomasin, P.; Detalle, V.; Vallet, J.; Labouré, M.; Olteanu, I.; Favaro, M.; Chiurato, M.; Bernardi, A.; Becherini, F. Calcium alkoxides as alternative consolidants for wall paintings: Evaluation of their performance in laboratory and on site, on model and original samples, in comparison to conventional products. *J. Cult. Herit.* **2017**, *29*, 54–56. [[CrossRef](#)]
21. Ibrahim, M.; Mohamed, S.; Hefni, Y.; Ahmed, A. Nanomaterials for consolidation and protection of egyptian faience form Matteria, Egypt. *J. Nano Res.* **2019**, *56*, 39–48. [[CrossRef](#)]
22. Zhu, J.; Li, X.; Zhang, Y.; Wang, J.; Wei, B. Graphene-enhanced nanomaterials for wall painting protection. *Adv. Funct. Mater.* **2018**, *28*, 1803872. [[CrossRef](#)]
23. Lai, W.H.; Wang, Y.X.; Wang, Y.; Wu, M.; Wang, J.Z.; Liu, H.K.; Chou, S.L.; Chen, J.; Dou, S.X. Morphology tuning of inorganic nanomaterials grown by precipitation through control of electrolytic dissociation and supersaturation. *Nat. Chem.* **2019**, *11*, 695–701. [[CrossRef](#)] [[PubMed](#)]
24. Rodrigues, J.D.; Grossi, A. Indicators and ratings for the compatibility assessment of conservation actions. *J. Cult. Herit.* **2007**, *8*, 32–43. [[CrossRef](#)]